

UniHDA: Towards Universal Hybrid Domain Adaptation of Image Generators

Hengjia Li¹ Yang Liu¹ Yuqi Lin¹ Zhanwei Zhang¹ Yibo Zhao¹ Weihang Pan¹
 Tu Zheng² Zheng Yang² Chunjiang Yu³ Boxi Wu¹
 Deng Cai¹

¹ Zhejiang University ² Fabu Inc. ³ Ningbo Port



Figure 1. Application of UniHDA. Given a pre-trained source generator and multiple target domains (either in text or image modalities), UniHDA adapts the generator to a hybrid target domain that blends all characteristics and maintains strong consistency with source domain.

Abstract

Generative domain adaptation has achieved remarkable progress, enabling us to adapt a pre-trained generator to a new target domain. However, existing methods simply adapt the generator to a single target domain and are limited to a single modality, either text-driven or image-driven. Moreover, they are prone to overfitting domain-specific attributes, which inevitably compromises cross-domain consistency. In this paper, we propose UniHDA, a unified and versatile framework for generative hybrid domain adaptation with multi-modal references from multiple domains. We use CLIP encoder to project multi-modal references into a unified embedding space and then linear interpolate the direction vectors from multiple target domains to achieve hybrid domain adaptation. To ensure the cross-domain consistency, we propose a novel cross-domain spatial structure (CSS) loss that maintains detailed spatial structure information between source and target generator. Experiments show

that the adapted generator can synthesise realistic images with various attribute compositions. Additionally, our framework is versatile to multiple generators, e.g., StyleGAN2 and Diffusion Models.

1. Introduction

Benefiting from tremendous success of modern image generator [1, 8, 25, 31], generative domain adaptation has achieved remarkable progress during the past few years. Typically, it aims to adapt a pre-trained generator to a new target domain while preserving the variation in the source domain, e.g., from the *human* domain to the *baby* domain. Depending on the modality of references, generative domain adaptation can be categorized into two schools: text-driven [5, 17] and image-driven [14–16, 19, 35, 40].

Despite their promising results, there are still some limitations. A major limitation of existing methods is that they

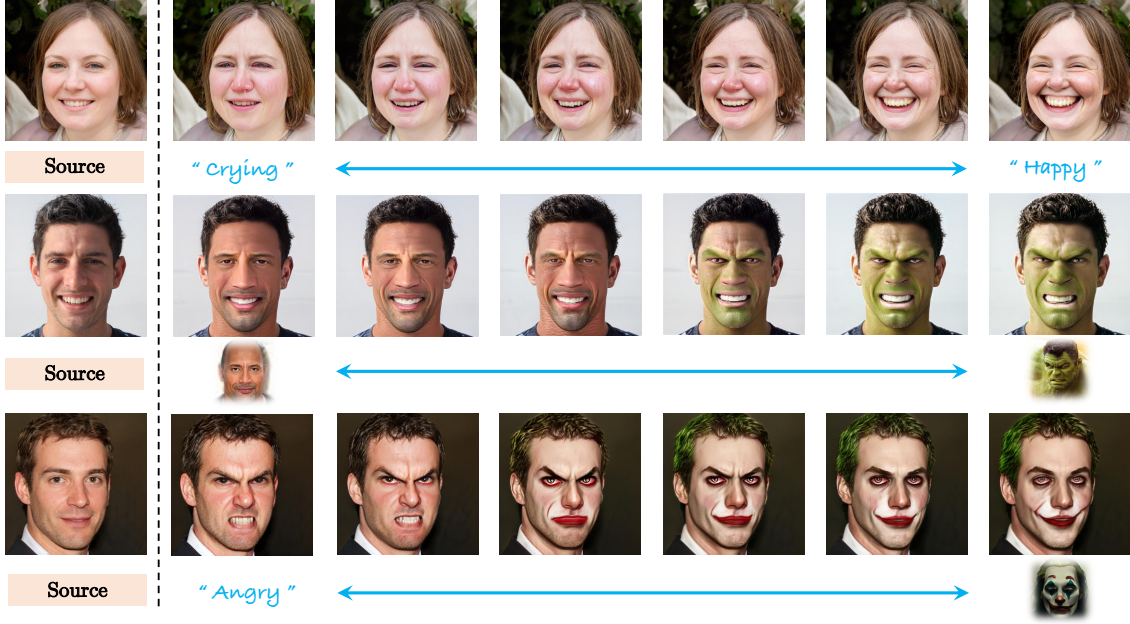


Figure 2. Linear interpolation between multi-modal direction vectors. We represent the domain shift by the direction vector from source embedding to the target (e.g., *Crying* or *Happy*). Linear interpolation of them during training will result in a smooth traversal.

only support adaptation from a source domain to individual target domain. These methods fail to directly adapt a *human* generator to more practical real-world scenarios like *angry person with the style of sketch* or a combination of *Johnson* and *Elena* (Fig. 1). For more general purposes, previous methods also fail with multi-modal references, e.g., *smiling Joker* given the *non-smiling Joker* image and the *smile* text.

Another limitation of existing approaches is that, in the pursuit of faithful adaptation, they are prone to overfit domain-specific attributes, especially in image-driven scenarios [19]. This inevitably compromises cross-domain consistency and impedes the inheritance of the diversity from the source generator.

In this paper, we propose UniHDA, a **U**niversal framework for generative **H**ybrid **D**omain **A**daptation with multi-modal references from multiple domains. UniHDA facilitates the reference of individual image and text prompt simultaneously and blends the attributes from diverse target domains to create a hybrid domain. To enable multiple modalities, we leverage pre-trained CLIP [24] to project multi-modal references into a unified embedding space and represent the domain shift by the direction vector from the source embedding to the target embeddings.

To achieve hybrid domain adaptation, we draw inspiration from the compositional capabilities in the latent space of StyleGAN [6, 27, 36]. We demonstrate that a semantically meaningful linear interpolation between two direction vectors in CLIP’s embedding space can uncover favorable compositional capabilities, as shown in Fig. 2. In light of this intriguing finding, we linearly interpolate direction vectors

of multiple target domains to obtain the direction vector corresponding to the hybrid domain that semantically integrates attributes from all target domains.

Furthermore, we introduce a novel cross-domain spatial structure loss (CSS) to preserve the consistency between source and target generator by maintaining detailed spatial structure information. Concretely, we leverage pre-trained DINO-ViT [4, 21] to encode generated images into patch tokens with fine-grained spatial information. For cross-domain consistency, we maintain the correspondence between source and target tokens with contrastive learning [20].

We conduct experiments for a wide range of source and target domains to validate the effectiveness of our method. Results demonstrate that the adapted generator can synthesise realistic images with various attribute compositions. In addition, we show that UniHDA is agnostic to the type of generators (e.g., StyleGAN2 [8–10] and Diffusion models [7, 11]). Our contributions are as follows:

- We propose a unified and versatile framework for generative domain adaptation, which enables multi-modal references and hybrid target domain, e.g., text-text, image-image, and image-text.
- We demonstrate strong compositional capabilities of direction vectors in CLIP’s embedding space. Taking advantage of it, we propose to linearly interpolate the direction vectors for hybrid domain adaptation.
- We propose a cross-domain spatial structure loss to maintain fine-grained spatial structure information between source and target generator, which significantly improves cross-domain consistency.

- We demonstrate successful multi-modal hybrid domain adaptation to diverse new domains for various generators and illustrate its advantage over other methods.

2. Related Work

Text-driven Generative Domain Adaptation. Text-driven domain adaptation involves using a textual prompt to shift the domain of a pre-trained model toward a new domain. For example, Style-NADA [5] presents a local direction CLIP [24] loss to align the embeddings of the generated images and text. Based on Style-NADA, Domain Expansion (DE) [18] proposes to expand the generator to jointly model multiple domains with texts.

Image-driven Generative Domain Adaptation. Image-driven generative domain adaptation refers to the adaptation of a pre-trained image generator to a new target domain using a limited number of training images. Due to the scarcity of training images, prior researches [14–16, 19, 33, 35, 39–41] often integrate additional regularization terms to prevent overfitting. For instance, CDC [19] introduces the instance distance consistency loss to maintain the distance between different instances in the source domain. Although these researches have made significant strides in generative domain adaptation, they heavily rely on the discriminator, making it challenging to handle hybrid domain adaptation.

Generative Hybrid Domain Adaptation. To combine multiple domains and achieve hybrid domain adaptation, several domain adaptation methods propose to train a separate generative model per domain and combine their effects in test-time, *e.g.*, Style-NADA [5]. Although having potential for hybrid domain adaptation, it doubles the model size and training time due to the requirement for training multiple models separately. Domain Expansion (DE) [18] proposes to expand the generator to jointly model multiple domains via decompose latent space. However, it requires the source dataset (*e.g.*, FFHQ [8]) for regularization, which significantly increases training time. Furthermore, it relies on the semantic latent space of the generator (*e.g.*, StyleGAN [8] and DiffAE [23]) for hybrid domain adaptation, limiting its applicability to a broader range of generators. Recently, FHDA [13] proposes few-shot hybrid domain adaptation and introduces a directional subspace loss to achieve it. Differently, we focus on multi-modal references with the text and 1-shot image, which offers greater flexibility and versatility.

Disentanglement in Generative Models. As observed in StyleGAN [8], the latent space is essentially a linear subspace. Recent works [6, 22, 27, 28, 30, 32, 34, 36] propose to find individual latent factors for image variations. Among them, SeFa [27] computes the eigenvalues of the transformation matrix to find the latent directions. As for diffusion models, DiffAE [23] explores the possibility of using DPMs for representation learning and seeks to extract a meaningful and decodable representation of an input image via autoen-

coding. Drawing inspiration from the disentanglement in the latent space of them, we demonstrate that a semantically meaningful linear interpolation between the direction vectors in CLIP’s embedding space can similarly uncover favorable compositional capabilities, which facilitates us to achieve hybrid domain adaptation.

3. Method

3.1. Multi-Modal Hybrid Domain Adaptation

We start with a pre-trained generator G_S (*e.g.*, StyleGAN [8–10] and Diffusion model [7, 29]), that maps from noise z to images in a source domain \mathcal{S} . Given a new target domain \mathcal{T} referenced by texts [5, 11, 12, 38] or images [14–16, 19, 35, 40], generative domain adaptation aims to adapt G_S to yield a target generator G_T , which can generate images similar to domain \mathcal{T} .

Despite the promising results of existing methods, a major limitation of them is that they only support adaptation from the source domain to individual target domains and fail to directly adapt the generator to the hybrid domain which blends the characteristics of multiple domains. Furthermore, they fail with multi-modal adaptation driven by texts and images simultaneously.

For more general purposes, we propose multi-modal hybrid domain adaptation. Given N domains $\{\mathcal{T}_i\}_{i=1}^N$ with 1-shot image $\{Y_i\}$ and M domains $\{\mathcal{T}_j\}_{j=1}^M$ with the text prompt $\{P_j\}$, it aims to adapt the source generator G_S to G_T that models the hybrid domain $\mathcal{T} = \{\mathcal{T}_i\} \cup \{\mathcal{T}_j\}$ and generates images with integrated characteristics. To the end, we introduce UniHDA, a unified and versatile framework for multi-modal hybrid domain adaptation, as shown in Fig. 3.

3.2. Multi-modal Direction Loss

To enable multiple modalities, we leverage pre-trained CLIP [24] to encode text-image references into a unified semantic embedding space. Drawing inspiration from CLIP-based methods [5, 11, 12, 38], we represent the *domain shift* as the direction vector Δf_{dom} from the source embedding and the target embedding. For image reference Y_i and its CLIP embedding f_i , the *domain shift* is calculated by

$$\Delta f_{dom} = f_i - \bar{f}_s, \quad (1)$$

where \bar{f}_s is the mean embedding of several samples generated by G_S . For text prompt P_j and its CLIP embedding f_j ,

$$\Delta f_{dom} = f_j - \tilde{f}_s, \quad (2)$$

where \tilde{f}_s is the embedding of the source text prompt.

To adapt G_S , we initialize a new generator G_T from G_S and finetune it by aligning the *sample-shift* direction Δf_{smp}

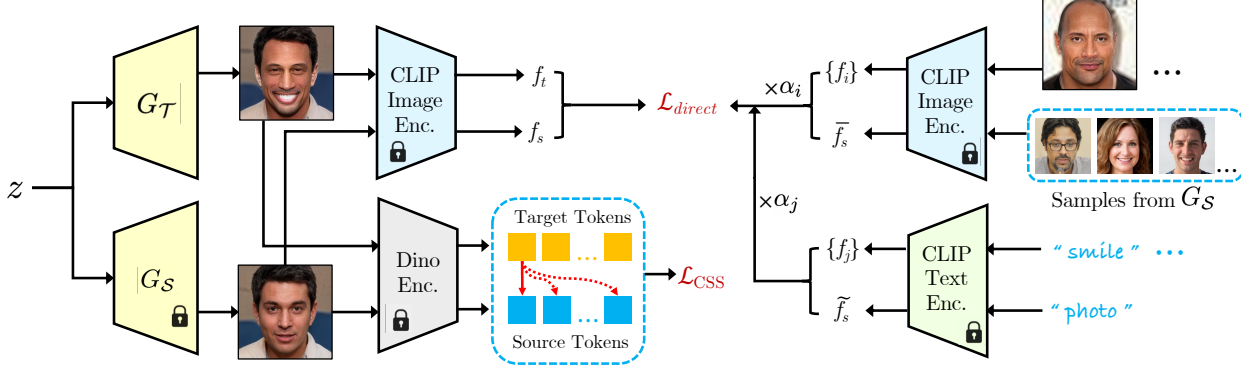


Figure 3. Overview of UniHDA with multi-modal direction loss \mathcal{L}_{direct} and cross-domain spatial structure loss \mathcal{L}_{CSS} . Utilizing CLIP image encoder and text encoder, \mathcal{L}_{direct} encourages $G_{\mathcal{T}}$ to faithfully acquire domain-specific characteristics with multi-modal references. To facilitate diversity inherited from $G_{\mathcal{S}}$, \mathcal{L}_{CSS} improves cross-domain consistency by maintaining detailed spatial structure information. The red solid line represents positive pairs, while red dashed lines represent negative pairs.

with the *domain-shift* direction Δf_{dom} . Formally,

$$\Delta f_{smp} = f_t - f_s, \quad (3)$$

$$\mathcal{L}_{direct} = 1 - \frac{\Delta f_{smp} \cdot \Delta f_{dom}}{\|\Delta f_{smp}\| \|\Delta f_{dom}\|},$$

where f_s and f_t are the embeddings of samples generated by $G_{\mathcal{S}}$ and $G_{\mathcal{T}}$ with the same noise.

3.3. Linear Composition of Direction Vectors

To achieve the hybrid domain adaptation, we draw inspiration from the compositional capabilities in the latent space of StyleGAN [6, 27, 36]. We illustrate that a linear interpolation between two direction vectors in the embedding space of CLIP, which is semantically meaningful, reveals promising compositional capabilities. As shown in Fig. 2, we can smoothly interpolate between two direction vectors calculated by distinct target prompts and source prompt “photo”, resulting in a gradual adaptation toward the target domain.

In light of this intriguing finding, we employ linear interpolation on the direction vectors of multi-modal target domains, to derive a consolidated direction vector representing the hybrid domain that seamlessly integrates all attributes semantically. For given domain coefficients $\{\alpha_i\}$ and $\{\alpha_j\}$, we obtain the direction vector

$$\Delta f_{dom} = \sum_{i=1}^N \alpha_i (f_i - \bar{f}_s) + \sum_{j=1}^M \alpha_j (f_j - \tilde{f}_s), \quad (4)$$

which represents the *domain shift* between the hybrid domain and source domain. We then substitute Eq. (4) into Eq. (3) to adapt $G_{\mathcal{S}}$ to the hybrid domain.

3.4. Cross-domain Spatial Structure Loss

Albeit the direction loss achieves multi-modal hybrid domain adaptation, the adapted generator are prone to over-

fit domain-specific attributes. This exacerbates when it comes to image-image and image-text scenarios owing to the scarcity of the images. To address this issue, we introduce a novel cross-domain spatial structure loss (CSS) to enhance cross-domain consistency, ensuring the preservation of intricate spatial structural information between the source and target generator.

Specifically, we leverage the pre-trained DINO-ViT [4, 21] to encode the generated images into patch tokens, containing detailed spatial structural information. DINO-ViT is self-supervised trained to focus on the distinction between subjects of the same class [26], which facilitates us to maintain the cross-domain consistency. Motivated by contrastive learning [20], we reduce the distance between the positive token pairs at the same position and push away the negative token pairs at the other positions by

$$\mathcal{L}_{CSS} = - \sum_i \log \frac{\exp(v_i^t \cdot v_i^s)}{\sum_j \exp(v_i^t \cdot v_j^s)}, \quad (5)$$

where v_i^t and v_j^s are the i -th and j -th tokens in the last layer of DINO-ViT from $G_{\mathcal{T}}$ and $G_{\mathcal{S}}$ respectively. The dot mark \cdot represents cosine similarity.

Overall, our training loss consists of two terms, i.e., the multi-modal direction loss \mathcal{L}_{direct} to achieve multi-modal hybrid domain adaptation and the cross-domain spatial structure loss \mathcal{L}_{CSS} to maintain cross-domain consistency:

$$\mathcal{L}_{overall} = \mathcal{L}_{direct} + \lambda \mathcal{L}_{CSS}, \quad (6)$$

where we use $\lambda = 5$ in our experiments.

4. Experiments

4.1. Experimental Setting

Methodology. We demonstrate the versatility of UniHDA on multi-modal hybrid domain adaptation, i.e., text-text, image-

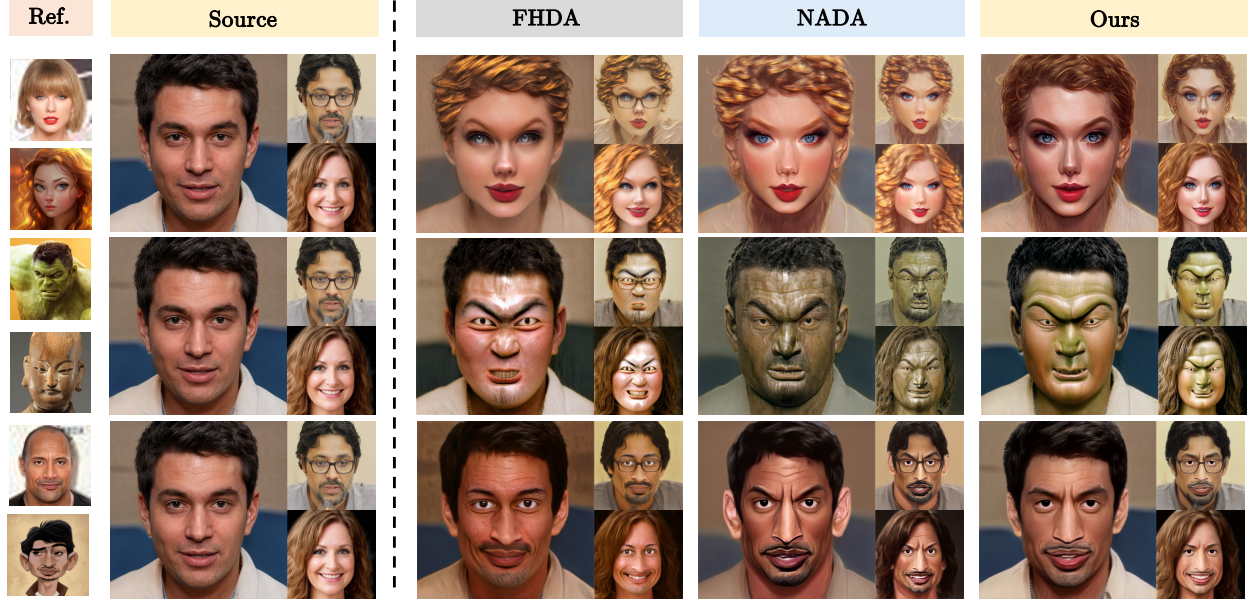


Figure 4. **Image-image** hybrid domain adaptation. We compare the results of FHDA [13], NADA [5] and UniHDA (Ours) with the same noise. FHDA and NADA generate images with poor cross-domain consistency, leading to a limited diversity. In contrast, UniHDA alleviates overfitting and maintains strong cross-domain consistency.

Method	<i>Taylor-Elena</i>		<i>Hulk-Wooden</i>		<i>Johnson-Comic</i>	
	CS-I (↑)	SCS (↑)	CS-I (↑)	SCS (↑)	CS-I (↑)	SCS (↑)
FHDA	0.685	0.576	0.635	0.659	0.640	0.679
NADA	0.684	0.579	0.624	0.575	0.647	0.642
Ours	0.699	0.738	0.649	0.707	0.656	0.764

Table 1. Quantitative results for **image-image** domain adaptation.

Method	<i>Baby-Red hair</i>		<i>Baby-Happy</i>		<i>Big-Blue eyes</i>	
	CS-T (↑)	SCS (↑)	CS-T (↑)	SCS (↑)	CS-T (↑)	SCS (↑)
DE	0.163	0.638	0.160	0.580	0.195	0.662
NADA	0.179	0.661	0.170	0.642	0.186	0.731
Ours	0.186	0.744	0.175	0.757	0.197	0.765

Table 2. Quantitative results for **text-text** domain adaptation.

image, and image-text. To show the generator-agnostic nature of UniHDA, we apply it to two well-known generators, *i.e.*, StyleGAN2 [9] and Diffusion model [11]). Following previous generative domain adaptation literatures [5, 14–16, 18, 19, 35, 38, 40], we use StyleGAN2 for comparisons in most experiments.

Datasets. We conduct the experiments for a wide range of source and target domains to validate the effectiveness of UniHDA. Following previous work, we consider FFHQ [8], AFHQ Dog [3], and LSUN Church [37] as the source domains. We adapt the pre-trained models to diverse hybrid domains driven by the text prompt and 1-shot image, where we set the domain coefficients in Eq. (4) as 0.5. Unless stated otherwise, we operate on 1024×1024 resolution images for both source and target domains.

Evaluation Metrics. One important aspect to evaluate generative domain adaptation is the preservation of domain-specific characteristics. Following [26], we use CLIP Score (CS-T and CS-I) for text-text and image-image adaptation

respectively. Concretely, CS-T is measured by the average cosine similarity between prompt and generated images’ embedding. CS-I is the average pairwise cosine similarity between CLIP embeddings of generated and real images. Here we use average CS-T or CS-I of multiple domains. Another important evaluation is the cross-domain consistency of the source domain. To measure it, we adopt Structural Consistency Score (SCS) [35] to evaluate the spatial structural consistency between source and target generator.

4.2. Image-image Hybrid Domain Adaptation

Fig. 4 shows the qualitative results of baselines and UniHDA for image-image adaptation. As shown in the figure, FHDA [13] suffers from severe model collapse and generates images with a limited diversity due to the scarcity of image references. While NADA [5] mitigates overfitting to a certain extent, its cross-domain consistency remains poor, resulting in the generation of similar images. In contrast, UniHDA maintains strong consistency and effectively

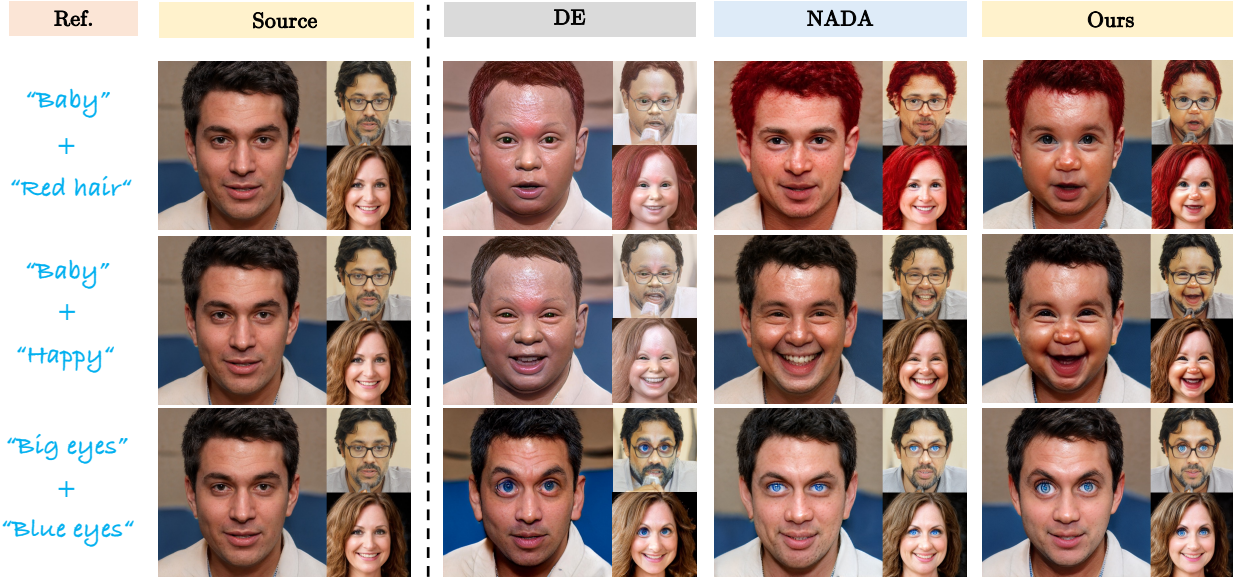


Figure 5. **Text-text** hybrid domain adaptation. We compare the results of DE [18], NADA [5] and UniHDA (Ours) with the same noise. UniHDA exhibits desirable performance to acquire characteristics from hybrid target domain and maintain robust cross-domain consistency.

generates images with characteristics of the hybrid domain.

We also quantitatively compare UniHDA with baselines. As shown in Tab. 1, ours clearly outperforms other methods. We achieve better CS-I and SCS, indicating that generated images effectively integrate domain-specific attributes and preserve primary characteristics of the source domain.

4.3. Text-text Hybrid Domain Adaptation

Fig. 5 shows the qualitative results of the baselines and UniHDA for text-text adaptation, all of which start from the same source domain FFHQ [8] to the combinations of individual domains. Since the adaptation is conducted solely along one projection direction of the latent code, Domain Expansion (DE) [18], to some extent, does not fully capture the characteristics of the target domain, *e.g.*, *baby* (Row 1 and Row 2). Furthermore, DE does not maintain robust cross-domain consistency, *e.g.*, the chin of the person in the upper-right corner and background artifacts in the Row 3. This is primarily due to the characteristics bias introduced when projecting the latent code to the base subspace, making the images appear less authentic. The main problem of NADA [5] is overfitting. Hard-to-learn characteristics, *e.g.*, *baby* (Row 1 and Row 2) and *big eyes* (Row 3) may be overshadowed by other overfitted ones. In contrast, UniHDA (Ours) exhibits desirable performance to generate images with integrated characteristics while maintaining robust consistency with the source domain.

Similar to Sec. 4.2, we also compare UniHDA with the baselines quantitatively. As shown in Tab. 2, ours clearly outperforms the baselines, which are consistent with qual-

Method	Extra Data Dependency	Model Dependency	2-domain		10-domain	
			size (↓)	time (↓)	size (↓)	time (↓)
DE	Source dataset	Single-Model*	24M	20h	24M	20h
NADA	-	Multi-Models	48M	4min	240M	20min
Ours	-	Single-Model	24M	2min	24M	2min

* indicates that DE needs a semantic latent space of the generator.

Table 3. Comparison with DE [18] and NADA [5]. For extra data dependency, DE needs source dataset (*e.g.*, FFHQ [8]) that significantly increases the training time. Besides, DE requires a semantic latent space, which limits the generalization for more generators. For hybrid N -domains, NADA utilizes N adapted models and necessitates N times the model size and training time.

itative results in Fig. 5. For CS-T, UniHDA significantly outperforms other methods, indicating that generated images effectively integrate multiple characteristics from distinct domains. Furthermore, UniHDA achieves better SCS, which effectively maintains cross-domain consistency compared with baseline methods.

4.4. Image-text Hybrid Domain Adaptation

Fig. 6 shows the results of image-text adaptation. As depicted in Sec. 4.2, NADA is susceptible to overfitting, which retains poor cross-domain consistency. In contrast, UniHDA (Ours) achieves robust cross-domain consistency and generates diverse images in all scenarios. Furthermore, we showcase the results of image-text hybrid domain adaptation on dogs [3], and churches [37] in Fig. 7. We can clearly

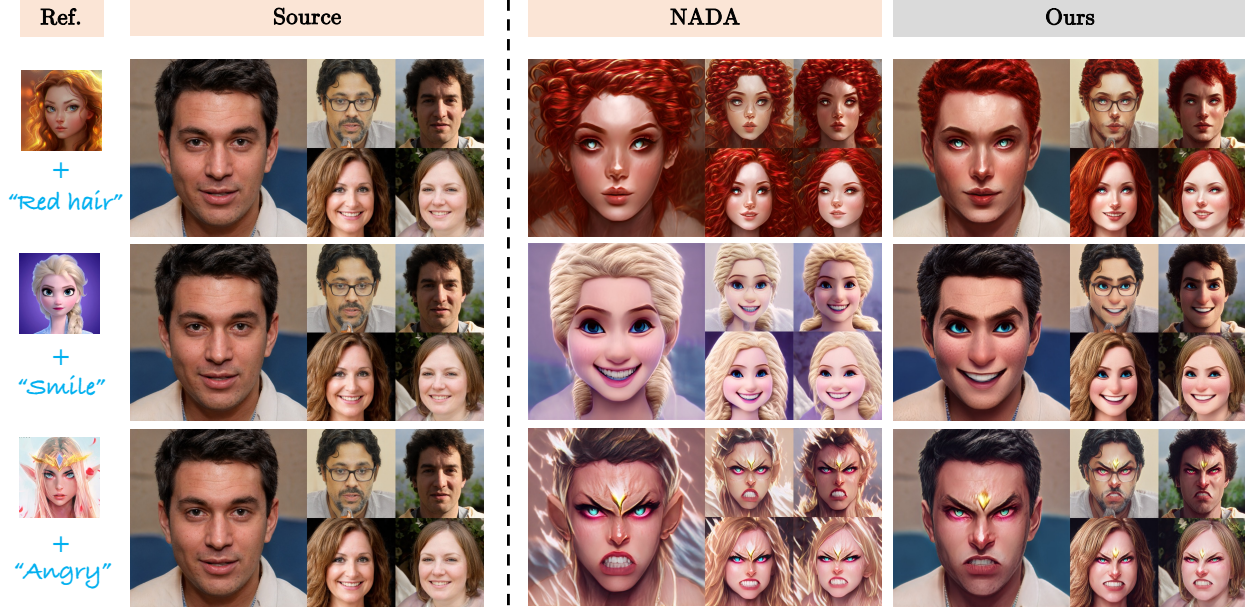


Figure 6. **Image-text** hybrid domain adaptation. Compared with NADA [5], UniHDA maintains strong cross-domain consistency.



Figure 7. Results of UniHDA for **image-text** hybrid domain adaptation on dogs [3], and churches [37]. The adapted generator can generate visually pleasant images with robust cross-domain consistency.

observe that it achieve desirable results across various target domains. More results are included in Appendix.

4.5. Comparison with Existing Methods

In Sec. 4.2 and Sec. 4.3, we find that while DE [18] and NADA [5] compromise cross-domain consistency, UniHDA (Ours) retains strong consistency and successfully captures the attributes of target domains. Besides, UniHDA also surpasses them in terms of efficiency, *e.g.*, model size and

training time as shown in Tab. 3. NADA trains a separate generative model per domain and interpolates their parameters in test-time, which necessitates multiple times the model size and training time. Although DE avoids cross-model interpolation, it heavily relies on the large source dataset (*e.g.*, FFHQ [8]) for regularization during training process, resulting in a significant increase in training time. In contrast, UniHDA circumvents these issues, which enables the completion of the adaptation within single generator and



Figure 8. Results of UniHDA with DiffusionCLIP [11]. We replace the training objective of DiffusionCLIP with our proposed \mathcal{L}_{direct} and \mathcal{L}_{CSS} . Results demonstrate that UniHDA is agnostic to the type of generators, allowing for its broader application on the diffusion model.

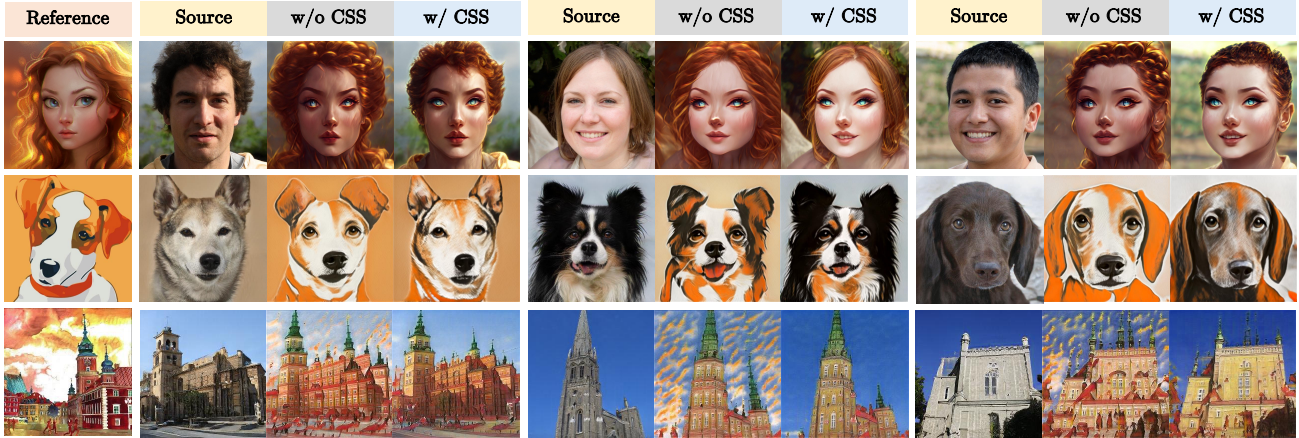


Figure 9. Ablation for our proposed \mathcal{L}_{CSS} on single domains, which significantly alleviates overfitting and improves cross-domain consistency.

only two minutes.

Additionally, DE relies on the semantic latent space of the generator (*e.g.*, StyleGAN [8] and DiffAE [23]) for hybrid domain adaptation, limiting its applicability to a broader range of generators. Conversely, UniHDA is not constrained by the type of generators, allowing for its broader application across various generators.

4.6. Generalization on Diffusion Models

In this section, we demonstrate that UniHDA is agnostic to the type of generative models and can easily generalize to diffusion models. Specifically, we apply UniHDA on DiffusionCLIP [11] and replace the training objective of DiffusionCLIP with our proposed \mathcal{L}_{direct} and \mathcal{L}_{CSS} . As shown in Fig. 8, the results work as well as those on StyleGAN2, which integrate the characteristics from multiple target domains and maintain robust consistency with the source domain. This verifies desirable generalization ability and versatility of UniHDA.

4.7. Effective of CSS Loss

We conduct the ablation study to evaluate the effects of our proposed Cross-domain Spatial Structure (CSS) loss on

single domains. As shown in Fig. 9, the results without \mathcal{L}_{CSS} suffer from overfitting and have very limited cross-domain consistency, *e.g.*, distorted backgrounds in Row 1 and 3. Benefited from CSS, the generated images maintain consistency with the source images in terms of spatial structure, thereby inheriting the diversity from the source domain. More results are included in Appendix.

5. Conclusion & Limitation

In this paper, we propose UniHDA, a unified and versatile framework for multi-modal hybrid domain adaptation. To enable multiple modalities, we leverage CLIP encoder to project multi-modal references into a unified embedding space. For hybrid domain, we demonstrate the compositional capabilities of direction vectors in CLIP’s embedding space and linearly interpolate direction vectors of multiple target domains. In addition, we propose a new cross-domain spatial structure loss to improve cross-domain consistency by preserving intricate spatial information between the source and target generators. We believe that our work is an important step towards generative domain adaptation since we have demonstrated that the source generator can be effectively

adapted to a hybrid domain with multi-modal references.

While UniHDA effectively realizes multi-modal hybrid domain adaptation, it also has the limitation. To encode both image and text into a shared embedding space, we utilize pre-trained CLIP during training time, which might bring potential bias for some domains. Nevertheless, we believe that the exploration of the novel task are significant for future work and solutions could be integrated into UniHDA to eliminate the bias.

References

- [1] Andrew Brock, Jeff Donahue, and Karen Simonyan. Large scale gan training for high fidelity natural image synthesis. In *ICLR*, 2018. 1
- [2] Eric R Chan, Connor Z Lin, Matthew A Chan, Koki Nagano, Boxiao Pan, Shalini De Mello, Orazio Gallo, Leonidas J Guibas, Jonathan Tremblay, Sameh Khamis, et al. Efficient geometry-aware 3d generative adversarial networks. In *Proceedings of the IEEE/CVF Conference on Computer Vision and Pattern Recognition*, pages 16123–16133, 2022. 1, 2
- [3] Yunjey Choi, Youngjung Uh, Jaejun Yoo, and Jung-Woo Ha. StarGAN v2: Diverse image synthesis for multiple domains. In *Proceedings of the IEEE/CVF Conference on Computer Vision and Pattern Recognition*, pages 8188–8197, 2020. 5, 6, 7
- [4] Alexey Dosovitskiy, Lucas Beyer, Alexander Kolesnikov, Dirk Weissenborn, Xiaohua Zhai, Thomas Unterthiner, Mostafa Dehghani, Matthias Minderer, Georg Heigold, Sylvain Gelly, et al. An image is worth 16x16 words: Transformers for image recognition at scale. *arXiv preprint arXiv:2010.11929*, 2020. 2, 4
- [5] Rinon Gal, Or Patashnik, Haggai Maron, Gal Chechik, and Daniel Cohen-Or. Stylegan-nada: Clip-guided domain adaptation of image generators. *arXiv preprint arXiv:2108.00946*, 2021. 1, 3, 5, 6, 7, 2
- [6] Erik Härkönen, Aaron Hertzmann, Jaakko Lehtinen, and Sylvain Paris. Ganspace: Discovering interpretable gan controls. *Advances in Neural Information Processing Systems*, 33:9841–9850, 2020. 2, 3, 4
- [7] Jonathan Ho, Ajay Jain, and Pieter Abbeel. Denoising diffusion probabilistic models. *Neural Information Processing Systems*, 2020. 2, 3
- [8] Tero Karras, Samuli Laine, and Timo Aila. A style-based generator architecture for generative adversarial networks. In *Proceedings of the IEEE/CVF conference on computer vision and pattern recognition*, pages 4401–4410, 2019. 1, 2, 3, 5, 6, 7, 8
- [9] Tero Karras, Samuli Laine, Miika Aittala, Janne Hellsten, Jaakko Lehtinen, and Timo Aila. Analyzing and improving the image quality of stylegan. In *Proceedings of the IEEE/CVF conference on computer vision and pattern recognition*, pages 8110–8119, 2020. 5
- [10] Tero Karras, Miika Aittala, Samuli Laine, Erik Härkönen, Janne Hellsten, Jaakko Lehtinen, and Timo Aila. Alias-free generative adversarial networks. *Advances in Neural Information Processing Systems*, 34:852–863, 2021. 2, 3
- [11] Gwanghyun Kim, Taesung Kwon, and Jong Chul Ye. Diffusionclip: Text-guided diffusion models for robust image manipulation. In *Proceedings of the IEEE/CVF Conference on Computer Vision and Pattern Recognition*, pages 2426–2435, 2022. 2, 3, 5, 8
- [12] Mingi Kwon, Jaeseok Jeong, and Youngjung Uh. Diffusion models already have a semantic latent space. *arXiv preprint arXiv:2210.10960*, 2022. 3
- [13] Hengjia Li, Yang Liu, Linxuan Xia, Yuqi Lin, Tu Zheng, Zheng Yang, Wenxiao Wang, Xiaohui Zhong, Xiaobo Ren, and Xiaofei He. Few-shot hybrid domain adaptation of image generators. *arXiv preprint arXiv:2310.19378*, 2023. 3, 5
- [14] Yijun Li, Richard Zhang, Jingwan (Cynthia) Lu, and Eli Shechtman. Few-shot image generation with elastic weight consolidation. In *Advances in Neural Information Processing Systems*, pages 15885–15896. Curran Associates, Inc., 2020. 1, 3, 5
- [15] Sangwoo Mo, Minsu Cho, and Jinwoo Shin. Freeze the discriminator: a simple baseline for fine-tuning gans. In *CVPR AI for Content Creation Workshop*, 2020.
- [16] Arnab Kumar Mondal, Piyush Tiwary, Parag Singla, and AP Prathosh. Few-shot cross-domain image generation via inference-time latent-code learning. In *The Eleventh International Conference on Learning Representations*. 1, 3, 5
- [17] Yotam Nitzan, Michaël Gharbi, Richard Zhang, Taesung Park, Jun-Yan Zhu, Daniel Cohen-Or, and Eli Shechtman. Domain expansion of image generators. 2023. 1
- [18] Yotam Nitzan, Michaël Gharbi, Richard Zhang, Taesung Park, Jun-Yan Zhu, Daniel Cohen-Or, and Eli Shechtman. Domain expansion of image generators. *arXiv preprint arXiv:2301.05225*, 2023. 3, 5, 6, 7, 2
- [19] Utkarsh Ojha, Yijun Li, Jingwan Lu, Alexei A Efros, Yong Jae Lee, Eli Shechtman, and Richard Zhang. Few-shot image generation via cross-domain correspondence. In *Proceedings of the IEEE/CVF Conference on Computer Vision and Pattern Recognition*, pages 10743–10752, 2021. 1, 2, 3, 5
- [20] Aaron van den Oord, Yazhe Li, and Oriol Vinyals. Representation learning with contrastive predictive coding. *arXiv preprint arXiv:1807.03748*, 2018. 2, 4
- [21] Maxime Oquab, Timothée Darcet, Théo Moutakanni, Huy Vo, Marc Szafraniec, Vasil Khalidov, Pierre Fernandez, Daniel Haziza, Francisco Massa, Alaaeldin El-Nouby, et al. Dinov2: Learning robust visual features without supervision. *arXiv preprint arXiv:2304.07193*, 2023. 2, 4
- [22] Or Patashnik, Zongze Wu, Eli Shechtman, Daniel Cohen-Or, and Dani Lischinski. Styleclip: Text-driven manipulation of stylegan imagery. In *Proceedings of the IEEE/CVF International Conference on Computer Vision*, pages 2085–2094, 2021. 3
- [23] Konpat Preechakul, Nattanat Chatthee, Suttisak Wizatwongsa, and Supasorn Suwajanakorn. Diffusion autoencoders: Toward a meaningful and decodable representation. In *Proceedings of the IEEE/CVF Conference on Computer Vision and Pattern Recognition*, pages 10619–10629, 2022. 3, 8
- [24] Alec Radford, Jong Wook Kim, Chris Hallacy, Aditya Ramesh, Gabriel Goh, Sandhini Agarwal, Girish Sastry, Amanda Askell, Pamela Mishkin, Jack Clark, et al. Learning

- transferable visual models from natural language supervision. In *International Conference on Machine Learning*, pages 8748–8763. PMLR, 2021. 2, 3
- [25] Robin Rombach, Andreas Blattmann, Dominik Lorenz, Patrick Esser, and Björn Ommer. High-resolution image synthesis with latent diffusion models. In *Proceedings of the IEEE/CVF Conference on Computer Vision and Pattern Recognition*, pages 10684–10695, 2022. 1
- [26] Nataniel Ruiz, Yuanzhen Li, Varun Jampani, Yael Pritch, Michael Rubinstein, and Kfir Aberman. Dreambooth: Fine tuning text-to-image diffusion models for subject-driven generation. In *Proceedings of the IEEE/CVF Conference on Computer Vision and Pattern Recognition*, pages 22500–22510, 2023. 4, 5
- [27] Yujun Shen and Bolei Zhou. Closed-form factorization of latent semantics in gans. In *Proceedings of the IEEE/CVF conference on computer vision and pattern recognition*, pages 1532–1540, 2021. 2, 3, 4
- [28] Yujun Shen, Ceyuan Yang, Xiaoou Tang, and Bolei Zhou. Interfacegan: Interpreting the disentangled face representation learned by gans. *IEEE transactions on pattern analysis and machine intelligence*, 44(4):2004–2018, 2020. 3
- [29] Jiaming Song, Chenlin Meng, and Stefano Ermon. Denoising diffusion implicit models. *arXiv: Learning, arXiv: Learning*, 2020. 3
- [30] Nurit Spingarn-Eliezer, Ron Banner, and Tomer Michaeli. Gan" steerability" without optimization. *arXiv preprint arXiv:2012.05328*, 2020. 3
- [31] Arash Vahdat, Karsten Kreis, and Jan Kautz. Score-based generative modeling in latent space. *Advances in Neural Information Processing Systems*, 34:11287–11302, 2021. 1
- [32] Andrey Voynov and Artem Babenko. Unsupervised discovery of interpretable directions in the GAN latent space. *arXiv preprint arXiv:2002.03754*, 2020. 3
- [33] Yi Wu, Ziqiang Li, Chaoyue Wang, Heliang Zheng, Shan-shan Zhao, Bin Li, and Dacheng Ta. Domain re-modulation for few-shot generative domain adaptation. *arXiv preprint arXiv:2302.02550*, 2023. 3
- [34] Zongze Wu, Dani Lischinski, and Eli Shechtman. StyleSpace analysis: Disentangled controls for StyleGAN image generation. *arXiv:2011.12799*, 2020. 3
- [35] Jiayu Xiao, Liang Li, Chaoferi Wang, Zheng-Jun Zha, and Qingming Huang. Few shot generative model adaption via relaxed spatial structural alignment. In *Proceedings of the IEEE/CVF Conference on Computer Vision and Pattern Recognition*, pages 11204–11213, 2022. 1, 3, 5
- [36] Guodong Xu, Yuenan Hou, Ziwei Liu, and Chen Change Loy. Mind the gap in distilling stylegans. In *Computer Vision—ECCV 2022: 17th European Conference, Tel Aviv, Israel, October 23–27, 2022, Proceedings, Part XXXIII*, pages 423–439. Springer, 2022. 2, 3, 4
- [37] Fisher Yu, Ari Seff, Yinda Zhang, Shuran Song, Thomas Funkhouser, and Jianxiong Xiao. Lsun: Construction of a large-scale image dataset using deep learning with humans in the loop. *arXiv preprint arXiv:1506.03365*, 2015. 5, 6, 7
- [38] Yabo Zhang, mingshuai Yao, Yuxiang Wei, Zhilong Ji, Jinfeng Bai, and Wangmeng Zuo. Towards diverse and faithful one-shot adaption of generative adversarial networks. In *Advances in Neural Information Processing Systems*, 2022. 3, 5
- [39] Yunqing Zhao, Keshigeyan Chandrasegaran, Milad Abdollahzadeh, and Ngai-Man Man Cheung. Few-shot image generation via adaptation-aware kernel modulation. *Advances in Neural Information Processing Systems*, 35:19427–19440, 2022. 3
- [40] Yunqing Zhao, Henghui Ding, Houjing Huang, and Ngai-Man Cheung. A closer look at few-shot image generation. In *Proceedings of the IEEE/CVF Conference on Computer Vision and Pattern Recognition*, pages 9140–9150, 2022. 1, 3, 5
- [41] Yunqing Zhao, Chao Du, Milad Abdollahzadeh, Tianyu Pang, Min Lin, Shuicheng Yan, and Ngai-Man Cheung. Exploring incompatible knowledge transfer in few-shot image generation. In *Proceedings of the IEEE/CVF Conference on Computer Vision and Pattern Recognition*, pages 7380–7391, 2023. 3

UniHDA: Towards Universal Hybrid Domain Adaptation of Image Generators

Supplementary Material

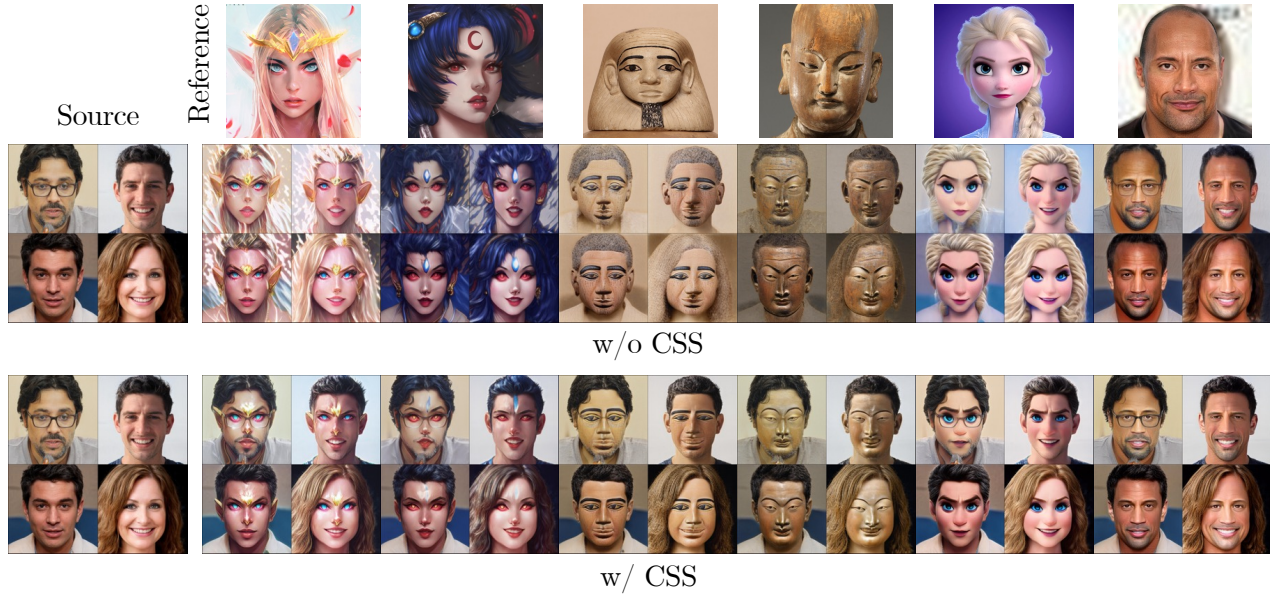


Figure 10. More qualitative results to verify the effectiveness of our proposed \mathcal{L}_{CSS} .

\mathcal{L}_{CSS}	Elena	Dog	Church
	0.569	0.429	0.617
✓	0.748	0.671	0.752

Table 4. Quantitative study of our \mathcal{L}_{CSS} , which significantly improves cross-domain consistency and achieves better SCS score.

6. Appendix

6.1. More Ablation of CSS Loss

As depicted in Sec. 4.7, our proposed \mathcal{L}_{CSS} significantly alleviates overfitting and improves cross-domain consistency. We conduct the quantitative study in Tab. 4, which aligns with the earlier qualitative results in Fig. 9. Results with \mathcal{L}_{CSS} achieve better SCS score, indicating that they maintain stronger consistency with the source domain. Additionally, we show more qualitative results in Fig. 10 to verify the effectiveness of UniHDA.

6.2. Hybrid Domain Adaptation of 3D Generator

To verify the versatility of UniHDA, We apply it on the popular 3D-aware image generation method, EG3D [2]. Specifically, we replace the discrimination loss with our proposed \mathcal{L}_{direct} and \mathcal{L}_{CSS} for hybrid domain adaptation. As shown in Fig. 11, the results effectively integrate the

attributes and preserve the characters and poses of source domain.

6.3. Results of Incompatible Domain Adaptation

To verify the generalization ability of UniHDA, we additionally conduct experiments for hybrid domain adaptation on incompatible domains, *i.e.* from *cat* to *rabbit*. As shown in Fig. 12 and Fig. 13, we start from AFHQ *cat* and *dog* to incompatible domains respectively. We can observe that the results effectively integrate the attributes of the corresponding domain and maintain robust consistency with source domain.

6.4. Effect of Encoder for CSS

We conduct experiments on pre-trained ViT, MViTv2, and Dinov2 to explore the impact of different image encoders for CSS. As shown in Fig. 14, Fig. 15, and Fig. 16, we showcase the results of image-image, text-text, and image-text respectively. We can observe that all of them improve the consistency with source domain compared with the baseline approach. Furthermore, they exhibit a similar qualitative style, which demonstrates that our CSS is agnostic to different pre-trained image encoders.



Figure 11. Hybrid domain adaptation in 3D generator. To show the versatility of UniHDA, we apply it on the popular 3D-aware generator, EG3D [2].

6.5. More Results for DiffusionCLIP

To demonstrate the versatility of UniHDA, we apply it on DiffusionCLIP in Sec. 4.6. As shown in Fig. 17, we showcase more results for DiffusionCLIP including image-image, text-text, and image-text. All results achieve hybrid domain adaptation and preserve strong corss-domain consistency.

6.6. More Qualitative Results

We apply UniHDA to adapt the generator on FFHQ to more hybrid domains, *i.e.*, text-text, image-image, and image-text. As shown in Fig. 18, Fig. 19, and Fig. 20, UniHDA successfully generates images with integrated characteristics from multiple target domains and maintains robust consistency with the source domain. Besides, we showcase more results of hybrid domain adaptation from AFHQ *dog* in Fig. 21.

6.7. Implement Details

Following the setting of previous generative domain adaptation methods [5, 18], we utilize the batch size of 4 and ADAM Optimizer with a learning rate of 0.002 for all experiments during training. A training session typically requires 300 iterations in 2 minutes, which significantly reduces training time compared with adversarial methods for generative domain adaptation. Note that we conduct all experiments on a single NVIDIA RTX 4090 GPU. [The code will be open source.](#)

For experiments on FFHQ, we generate images with 1024×1024 resolution. As for AFHQ-Dog and LSUN-Church, we operate on 512×512 and 256×256 resolution images respectively.



Figure 12. Hybrid domain adaptation from AFHQ *cat* to incompatible domains, *i.e.* *lion*, *rabbit*, and *tiger*.



Figure 13. Hybrid domain adaptation from AFHQ *dog* to incompatible domains, *i.e.* *lion*, *rabbit*, and *tiger*.

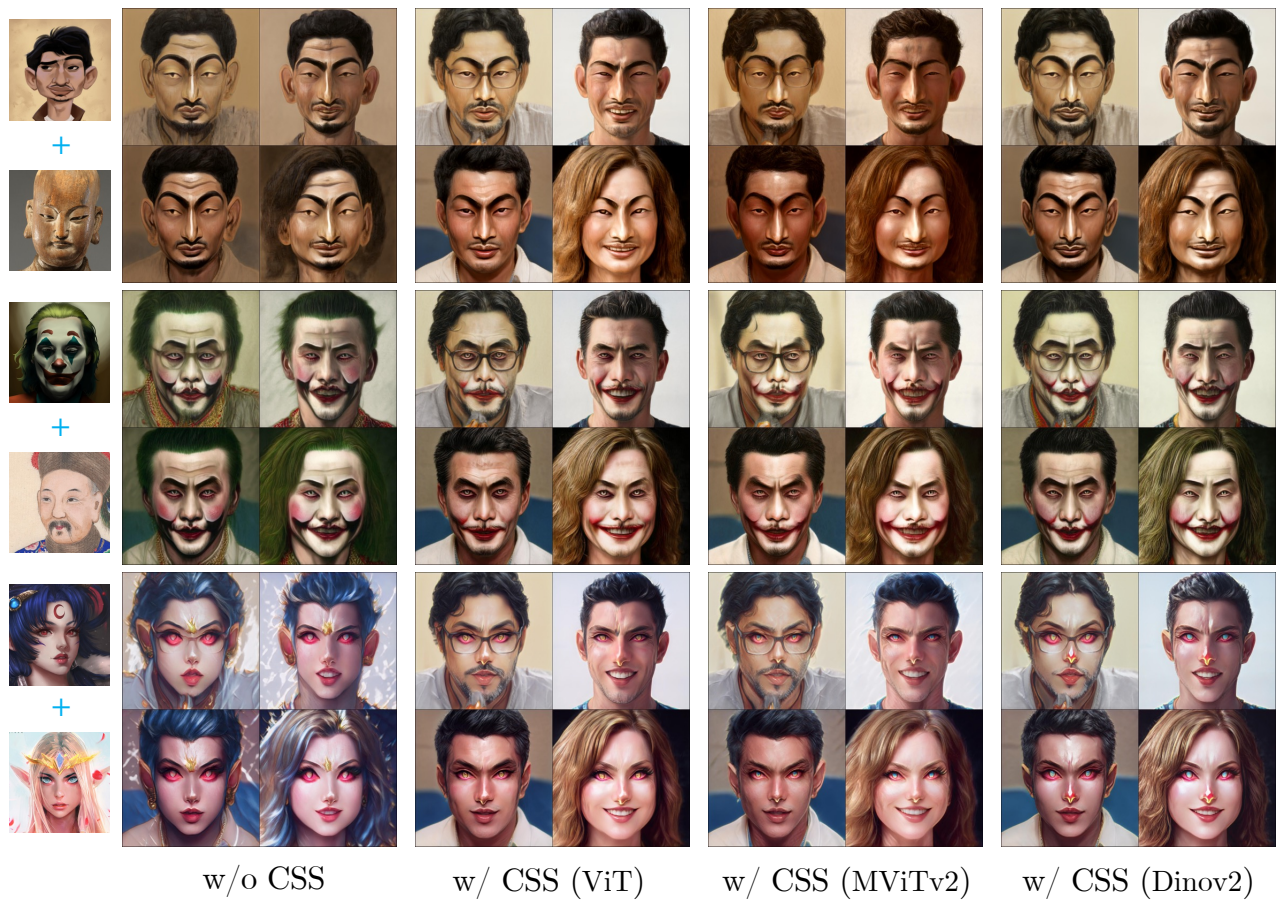


Figure 14. Effect of different pre-trained image encoders for CSS on image-image hybrid domain adaptation.



Figure 15. Effect of different pre-trained image encoders for CSS on text-text hybrid domain adaptation.

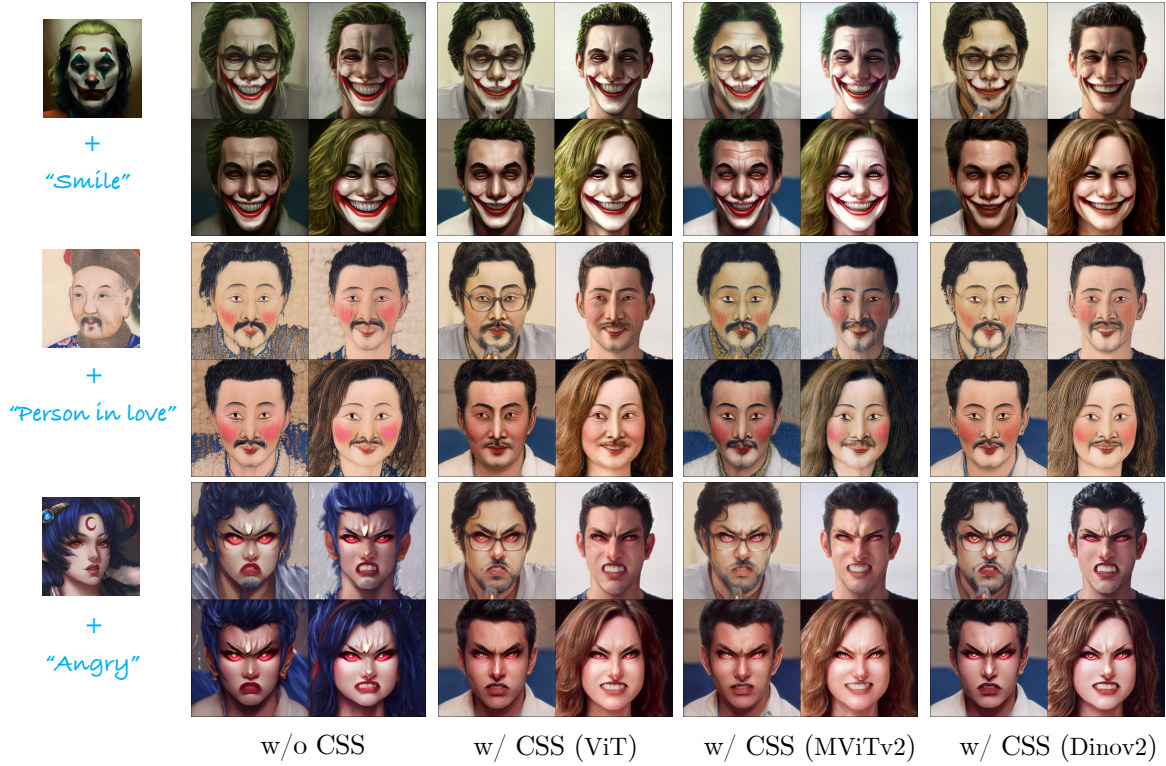


Figure 16. Effect of different pre-trained image encoders for CSS on image-text hybrid domain adaptation.

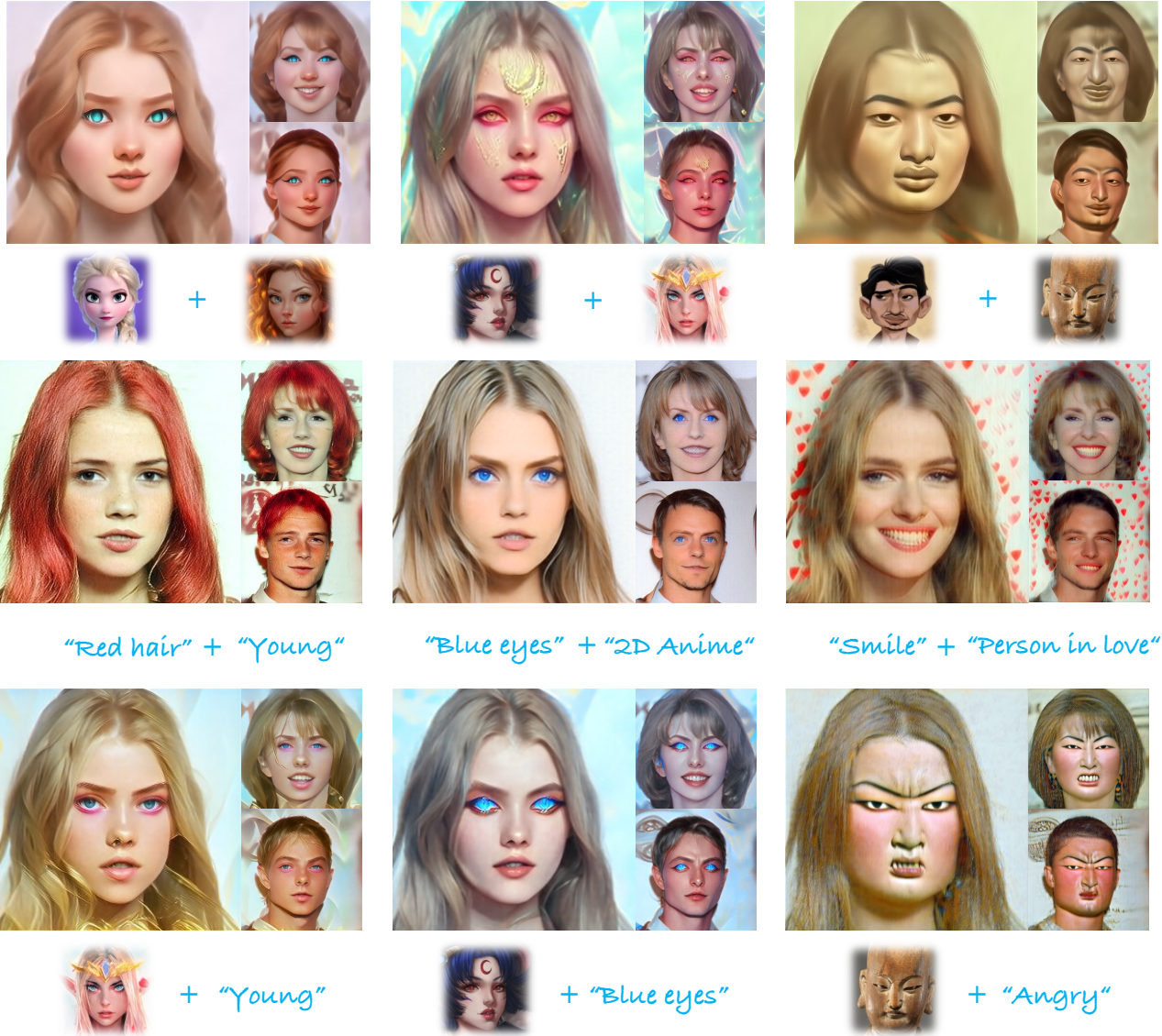


Figure 17. More results of UniHDA with DiffusionCLIP.



Figure 18. More results of image-image hybrid domain adaptation. The source image is in the top-left corner, and the first row and column consist of training images.

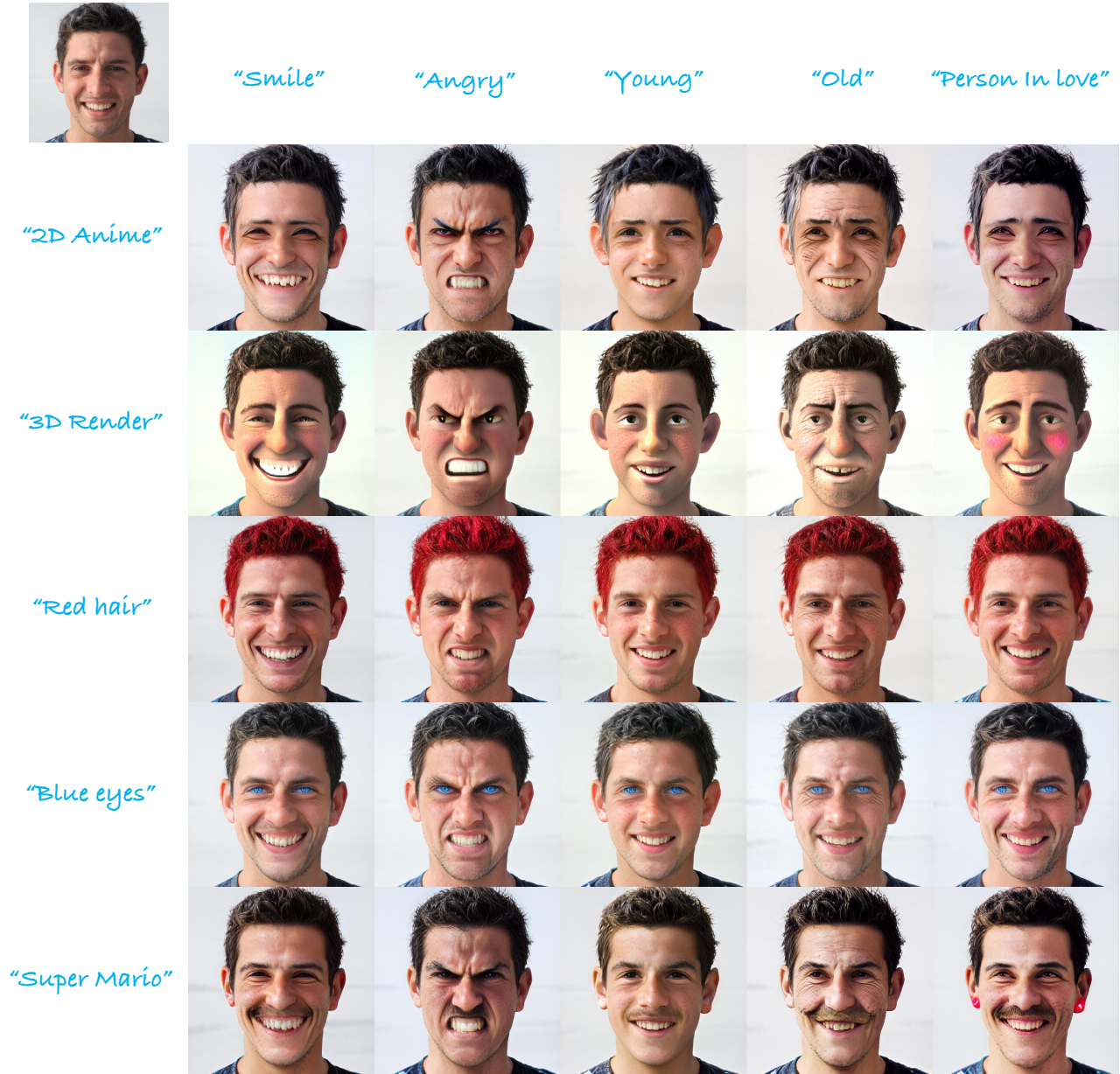


Figure 19. More results of text-text hybrid domain adaptation. The source image is in the top-left corner, and the first row and column consist of text prompts.

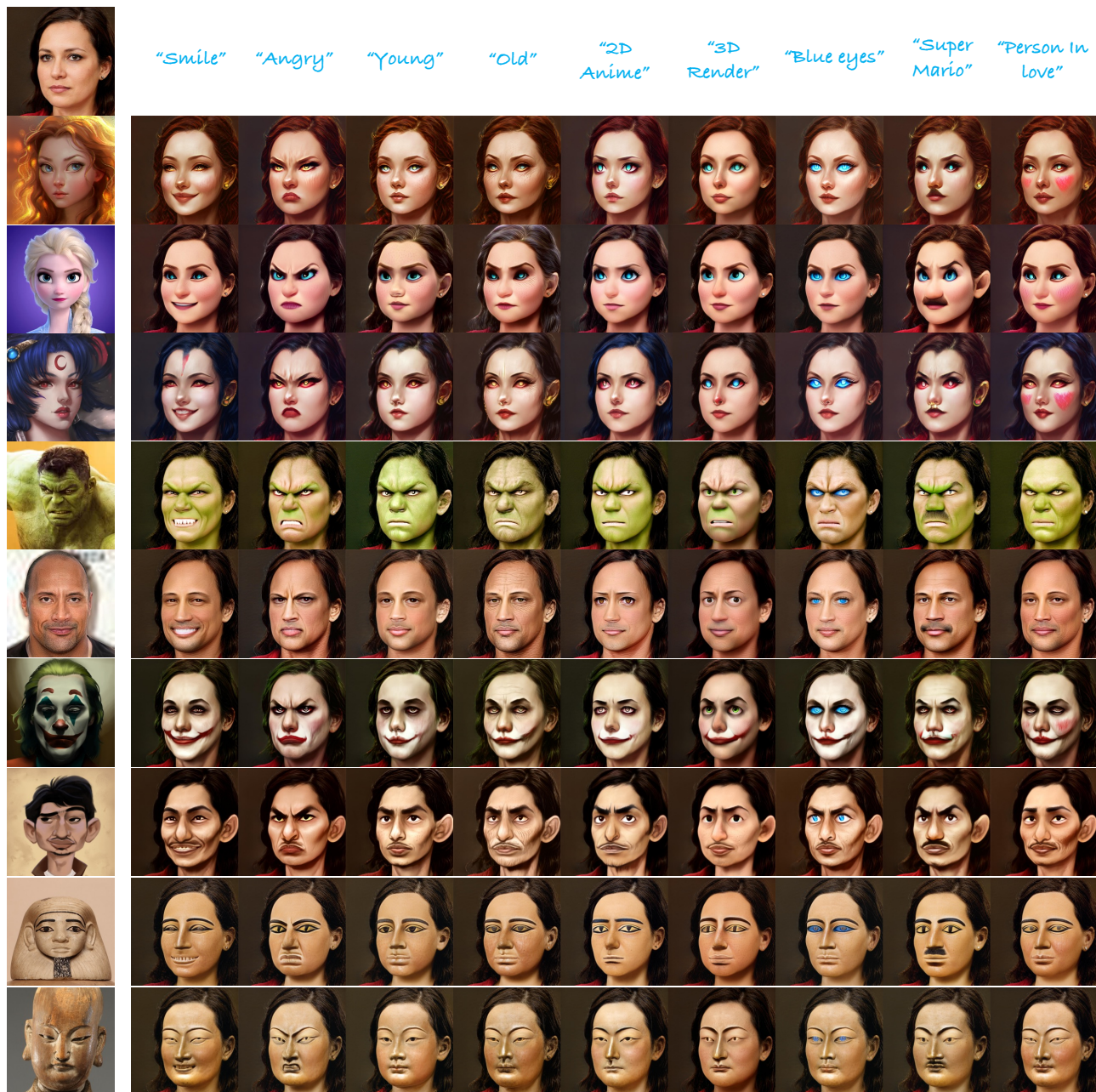


Figure 20. More results of image-text hybrid domain adaptation. The source image is in the top-left corner. The first row and column consist of training images and text prompts respectively.

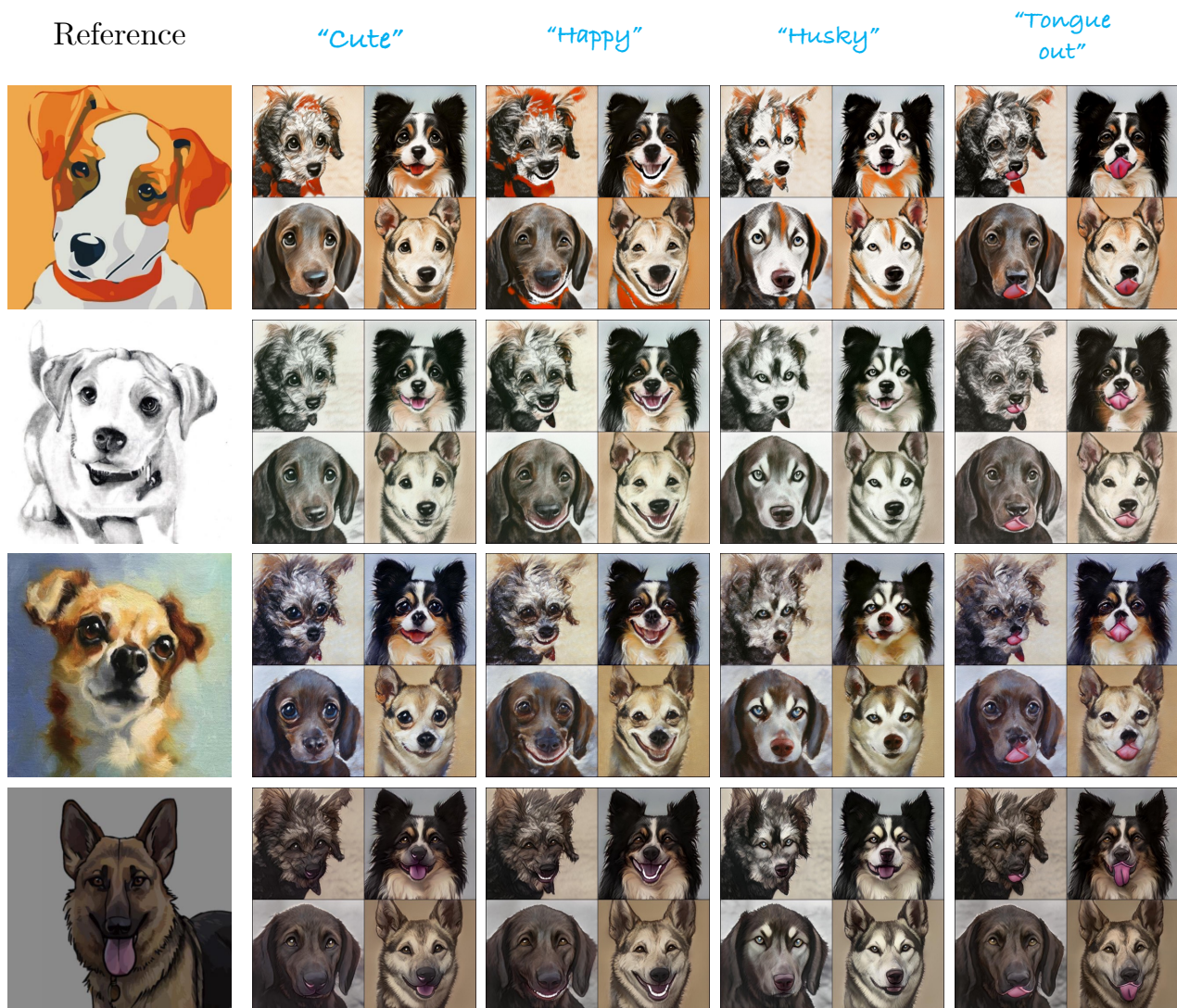


Figure 21. More results of image-text hybrid domain adaptation on AFHQ *dog*.